

See discussions, stats, and author profiles for this publication at: <https://www.researchgate.net/publication/8632065>

# Local Structure of the Zeolitic Catalytically Active Site during Reaction

ARTICLE *in* JOURNAL OF THE AMERICAN CHEMICAL SOCIETY · MAY 2004

Impact Factor: 12.11 · DOI: 10.1021/ja031755j · Source: PubMed

---

CITATIONS

38

---

READS

46

## 3 AUTHORS:



Jeroen A van Bokhoven

ETH Zurich

267 PUBLICATIONS 5,988 CITATIONS

SEE PROFILE



A.M.J. van der Eerden

Utrecht University

53 PUBLICATIONS 1,375 CITATIONS

SEE PROFILE



Roel Prins

ETH Zurich

425 PUBLICATIONS 12,980 CITATIONS

SEE PROFILE

## Local Structure of the Zeolitic Catalytically Active Site during Reaction

Jeroen A. van Bokhoven,\* Ad M. J. van der Eerden,<sup>†</sup> and Roel Prins

Swiss Federal Institute of Technology (ETH) Zurich, CH-8093, Zurich, Switzerland and Debye Institute, Utrecht University, Sorbonnelaan 16, Utrecht, The Netherlands

Received December 16, 2003; E-mail: j.a.vanbokhoven@tech.chem.ethz.ch

Zeolites are microporous alumina-silicates that are widely applied as selective sorbents and catalysts. Tetrahedrally coordinated aluminum atoms that are connected by a hydroxyl group to a neighboring silicon atom are the catalytically active centers in Brønsted-acid-catalyzed reactions.<sup>1</sup> Extensive characterization of the catalytically active site has been obtained using IR and NMR techniques. Thus far, however, the local structure of the catalytically active site during catalytic action has hardly been studied because of experimental limitations. Here we present the structural changes in the catalytically active centers during catalytic action by means of in situ Al K edge EXAFS analysis. It is shown that the strongly distorted tetrahedral aluminum in acidic zeolite partially relaxes after the adsorption of a reaction intermediate on the Brønsted acid site.

An activated dehydrated zeolite contains a heavily distorted tetrahedral site, and as a result, the aluminum experiences a large quadrupolar interaction, thus broadening the NMR resonance. This results in "NMR invisible aluminum"; only recently was the distorted tetrahedrally coordinated aluminum directly observed using DFS-enhanced <sup>27</sup>Al MQ MAS NMR.<sup>2</sup> Much insight into the aluminum structure came from theoretical calculations.<sup>3</sup> They indicate that the tetrahedrally coordinated aluminum contains one long and three short aluminum–oxygen bonds in acidic zeolites. Adsorption of bases on the Brønsted acid site decreases the tetrahedron distortion with increasing basicity.<sup>3b</sup>

The bridging hydroxyl group is strongly acidic and the catalytically active center for Brønsted acid-catalyzed reactions. Many catalytic reactions of hydrocarbons proceed via carbenium ion intermediates. However, theory has predicted that these ions are generally not present in zeolites as stable intermediates, like in superacid media, but that they are transition states.<sup>3c,4</sup> Instead, these ions form stable alkoxy species on the zeolitic aluminum tetrahedral sites. Experimental evidence from IR and NMR confirmed the presence of stable alkoxy intermediates on the catalytically active sites.<sup>5</sup> Scheme 1 shows the formation of such alkoxy species from an alkene on a Brønsted acid site.

An alkene adsorbs  $\pi$ -bonded to the Brønsted acid site below room temperature. At higher temperature, alkoxy species are formed. This is accompanied by oligomerization of the alkene, and bulky alkoxy species are formed.<sup>6</sup> At even higher temperatures, alkenes react further to yield coke, thus restoring the hydroxyl group.<sup>5c</sup> The reactivity of the alkenes depends on the nature of the alkene and on the structure of the zeolite.

Here, we present an in situ EXAFS study of the Al K edge on zeolite Y during the oligomerization of ethene. The local structure of the catalytically active site during the reaction is determined. Measurements were performed on beamline 3.4 of the SRS Daresbury (UK), which is equipped with a double-crystal monochromator using YB<sub>64</sub> crystals. NH<sub>4</sub>–Y zeolite with a Si/Al ratio of 2.6 (obtained from BP Amoco) was placed in an in situ cell,

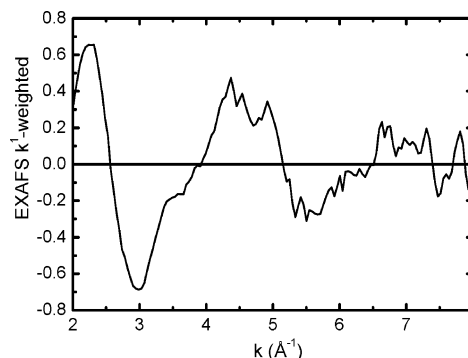
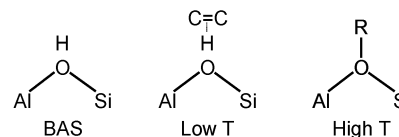


Figure 1.  $k^1$ -Weighted normalized Al K edge EXAFS data of NH<sub>4</sub>–Y zeolite.

Scheme 1. Oligomerization of an Alkene to a Bulky Alkoxy Species, R, on Zeolitic Brønsted Acid Sites (BAS)



especially designed for soft EXAFS,<sup>7</sup> and measured in a flow of helium that was dried by passing it through a cold trap. Standard background subtraction procedures<sup>8</sup> were performed using the XDAP data-analysis code.<sup>9</sup> Fits were performed in R-space. Theoretical references were obtained with the multiple-scattering code FEFF8.<sup>10</sup> Figure 1 shows the  $k^1$ -weighted isolated EXAFS data of NH<sub>4</sub>–Y. The quality of the data is sufficient to perform first-shell analyses. The data range is limited by the presence of the Si K edge at 1840 eV.

The structure and crystallinity of NH<sub>4</sub>–Y were checked with <sup>27</sup>Al and <sup>29</sup>Si MAS NMR, XRD, and N<sub>2</sub> physisorption, indicating that all aluminum was tetrahedrally coordinated. This coordination was the starting point for the EXAFS analysis. The spectrum of NH<sub>4</sub>–Y was fitted with one oxygen coordination shell keeping all parameters free (Table 1). An oxygen coordination number of 4 was obtained at a distance of 1.68 Å, confirming the tetrahedral coordination. In addition to the one-shell model, a two-shell model was the starting point of a refinement. The shell was split into two contributions, and the coordination numbers and distances were independently refined. Two similar coordination numbers were found at distances that varied by about 0.03 Å, which statistically belong to the same coordination shell. The one-shell fit is a good representation of the EXAFS data (Table 1), in full agreement with the NMR measurements.

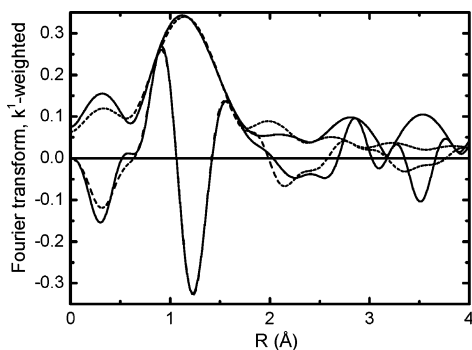
H–Y was obtained by removing ammonia by heating to 725 K in a flow of helium. During treatment, the in situ cell was cooled to prevent the fragile beryllium windows from heating. H–Y was measured at room temperature (H–Y (rt)). After this measurement, the flow was switched to 5% ethene in helium and EXAFS spectra were measured at various temperatures.

<sup>†</sup> Utrecht University.

**Table 1.** EXAFS Fit Results on Zeolite Y Measured at Various Temperatures in Helium or in Diluted Ethene Flow

sample	CN	$\Delta\sigma^2$	$R$ (Å)	$E_0$ (eV)	variance $k^1$ weighting
NH <sub>4</sub> -Y (rt)	4.4 <sup>a</sup>	0.000 <sup>b</sup>	1.68	-2.7	0.11 <sup>c</sup> 0.38 <sup>d</sup>
H-Y (rt)	3.1	-0.005	1.66	-3.1	0.45 <sup>c</sup> 0.85 <sup>d</sup>
H-Y C <sub>2</sub> = (323 K)	1.1	idem <sup>e</sup>	1.89	idem <sup>e</sup>	0.06 <sup>c</sup> 0.16 <sup>d</sup>
H-Y C <sub>2</sub> = (625 K)	3.4	-0.0037	1.64	-2.1	0.36 <sup>c</sup> 0.44 <sup>d</sup>
	1.1	idem <sup>e</sup>	1.81	idem <sup>e</sup>	
	2.9	-0.008	1.65	-3.9	
	1.1	idem <sup>e</sup>	1.91	idem <sup>e</sup>	

<sup>a</sup> Error margins coordination number  $\pm 15\%$ , distance  $\pm 0.025$  Å, Debye-Waller factor  $\pm 0.005$ . <sup>b</sup> Set to zero; other values are relative to this value. <sup>c</sup> Variance in imaginary part. <sup>d</sup> Variance in real part. <sup>e</sup> Same value forced for both shells.

**Figure 2.** Absolute and imaginary parts of the Fourier transform and best fit (dashed line) obtained for dehydrated H-Y zeolite using one long and three short Al-O bonds. The Fourier transform is  $k^1$ -weighted, and the Fourier range is  $2.74 < k < 8$  Å<sup>-1</sup>; the fit is performed in  $R$ -space:  $0 < R < 1.8$  Å.

The same procedure used for fitting the spectrum of NH<sub>4</sub>-Y was applied to all the other samples. In the case of H-Y, the two-shell model significantly improved the quality of the fit. Three short and one long aluminum-oxygen bonds were observed (Figure 2, Table 1). These results agree well with theoretical predictions<sup>3</sup> that indicate a larger aluminum-oxygen bond of about 0.2 Å to the oxygen that binds the proton. The proton-oxygen bond weakens the neighboring oxygen-aluminum bond. <sup>27</sup>Al MQ MAS NMR on dehydrated zeolite H-ZSM5 indicated a cylindrical symmetry of a heavily distorted tetrahedral aluminum,<sup>2</sup> which agrees with a model with one long and three short aluminum-oxygen bonds. Using Al K edge EXAFS spectroscopy, we established the local structure of the aluminum catalytically active site in zeolite H-Y.

Measuring H-Y zeolite in a flow of ethene in helium at 323 K gave a different result. Also in this case, the two-shell model gave the best fit. However, the long aluminum-oxygen bond was significantly shorter than in the case of H-Y zeolite: 1.81 versus 1.89 Å. This relaxation can be explained by the adsorption of a carbenium ion on the conjugated base of the Brønsted acid site forming the alkoxide species, formed by oligomerization of ethene (Scheme 1). It was shown previously that adsorption of a base on the acid site decreases the distortion of the tetrahedral aluminum.<sup>3b</sup> Hydrogen bonding of the base with the proton decreases the proton-oxygen bond strength, which increases the bonding between this oxygen and the aluminum. As a consequence, the tetrahedron becomes more symmetric. A limiting case occurs after the adsorption of a strong base, which causes a protonation of the base. As a

result, the four aluminum-oxygen bond lengths became very similar, as we measured for NH<sub>4</sub>-Y (Table 1). In our case, however, an alkene is adsorbed and reacts on the acid site, forming an alkoxy species. The formation of an oxygen-carbon bond weakens the aluminum-oxygen bond. However, the bond elongation is significantly less than in the case of the acidic zeolite. This was predicted by recent <sup>27</sup>Al NMR experiments, which indicated a lower quadrupolar coupling constant for the framework aluminum species in the case of an adsorbed alkoxy species compared to the bare acid site.<sup>11</sup>

An increase in temperature resulted in an elongation of the long aluminum-oxygen bond to a value comparable to that for H-Y zeolite. At the higher temperatures, coke formation occurs, which restores the bridging hydroxyl group.<sup>5c</sup> A highly asymmetric, tetrahedrally coordinated aluminum is obtained (Table 1). When samples that were treated above 325 K were removed from the in situ cell, they were covered by a black graphite-like layer. This confirms the extensive coking at these temperatures.

This study shows the power of EXAFS spectroscopy in resolving the local structure of the zeolitic catalytically active site during catalytic reaction. For the first time, the structural variation in the aluminum active site in zeolites during a catalytic reaction has been determined by in situ Al K edge EXAFS spectroscopy. We probed the local structure of the aluminum catalytically active site in H-Y zeolite and the changes that occur during the oligomerization reaction of an alkene. Application of in situ Al K edge spectroscopy is expected to provide further fundamental insight into the structure of zeolitic catalytically active sites during catalytic action.

**Acknowledgment.** Dr A. D. Smith is acknowledged for his help during the measurements. We thank the SRS Daresbury (UK) for providing beamtime (Beamtime Award Number 40203).

## References

- (1) Van Bakkum, H.; Flanigen, E. M.; Jacobs, P. A.; Jansen, J. C., Eds. *Introduction to Zeolite Science and Practice*, 2<sup>nd</sup> ed.; Elsevier: Amsterdam, 2001.
- (2) Kentgens, A. P. M.; Iagu, J.; Kalwei, M.; Koller, H. *J. Am. Chem. Soc.* **2001**, *123*, 2925.
- (3) (a) Eichler, U.; Brändle, M.; Sauer, J. *J. Phys. Chem. B* **1997**, *101*, 10035. (b) Eheresmann, J. O.; Wang, W.; Herreros, B.; Luigi, D.-P.; Venkatraman, T. N.; Song, W.; Nicholas, J. B.; Haw, J. F. *J. Am. Chem. Soc.* **2002**, *124*, 10868. (c) van Santen, R. A.; Kramer, G. *J. Chem. Rev.* **1995**, *95*, 637.
- (4) Kazansky, V. B.; Senchenya, I. N. *J. Catal.* **1989**, *119*, 108.
- (5) (a) Haw, J. F.; Richardson, B. R.; Oshiro, I. S.; Lazo, N. D.; Speed, J. A. *J. Am. Chem. Soc.* **1989**, *111*, 2052. (b) Stephanov, A. G. *Catal. Today* **1995**, *24*, 341. (c) Paze, C.; Sazak, B.; Zecchina, A.; Dwyer, J. *J. Phys. Chem.* **1999**, *103*, 9978.
- (6) (a) Stephanov, A. G.; Luzgin, M. V.; Romannikov, V. N.; Sidelnikov, V. N.; Paukshtis, E. A. *J. Catal.* **1998**, *178*, 466. (b) Haw, J. F.; Nicholas, J. B.; Xu, T.; Beck, L. W.; Ferguson, D. B. *Acc. Chem. Res.* **1996**, *29*, 259. (c) Ishikawa, H.; Yoda, E.; Kondo, J. N.; Wakabayashi, F.; Domen, K. *J. Phys. Chem. B* **1999**, *103*, 5681. (d) Spoto, G.; Bordiga, S.; Ricchiardi, G.; Scarano, D.; Zecchina, A.; Borello, E. *J. Chem. Soc., Faraday Trans.* **1994**, *90*, 2827.
- (7) (a) van Bokhoven, J. A.; van der Eerden, A. M. J.; Smith, A. D.; Koningsberger, D. C. *J. Synchrotron Radiat.* **1999**, *6*, 201. (b) van der Eerden, A. M. J.; van Bokhoven, J. A.; Smith, A. D.; Koningsberger, D. C. *Rev. Sci. Instrum.* **2000**, *71*, 3260.
- (8) Koningsberger, D. C.; Prins, R., Eds.; *X-ray Absorption: Principles, Applications, Techniques of EXAFS, SEXAFS and XANES* (John Wiley: New York, 1988).
- (9) Vaarkamp, M.; Linders, J. C.; Koningsberger, D. C. *Physica B* **1995**, *208* & *209*, 159.
- (10) Ankudinov, A. L.; Ravel, B.; Rehr, J. J.; Conradson, S. D. *Phys. Rev. B* **1998**, *58*, 7565.
- (11) Wang, W.; Buchholz, A.; Arnold, A.; Xu, M.; Hunger, M. *Chem. Phys. Lett.* **2003**, *370*, 88.

JA031755J